ELASTO-PLASTIC BEHAVIOR AND SEISMIC EVALUATION METHOD OF CONCRETE-FILLED SPIRAL STEEL PIPE PIERS

Kiyoshi Ono[1], Mitsuyoshi Akiyama[2], Masahiro Shirato[3] and Seiji Okada[4]

Abstract

Spiral steel pipes are relatively economical because they are produced in large quantities in factories. The application of spiral steel pipes to bridge piers is considered as one of the effective methods for decreasing construction cost of infrastructures. However, mechanical features of spiral steel pipes including seismic performance may be different from those of bending roll pipe piers. In this study, cyclic loading experiments were conducted for grasping the elasto-plastic behavior of concrete-filled spiral steel pipes piers. Furthermore, the experimental results were compared with previous experimental results and calculation results by the previous seismic evaluation method.

Introduction

It has been required to decrease the construction cost of infrastructures. Recently, methods like use of new materials and new structures for bridge construction have been proposed. By the way, spiral steel pipes have been mainly used as the foundations of buildings or bridges and they have been seldom used for bridge piers. The spiral steel pipes are manufactured in a factory line by continually unwinding a coil and molding it spirally into a cylindrical shape, with the joints being automatically welded. This enables production in large quantities, making spiral steel pipes relatively economical. Therefore, the application of spiral steel pipes to bridge piers has been considered as one of the effective methods. Moreover, by filling spiral steel pipes with concrete, it is thought that the seismic performance of spiral steel pipes piers can increase. However, roll forming processes of spiral steel pipes are different from those of bending roll pipes which are generally used as bridge piers. For this reason, elasto-plastic behavior of spiral steel pipes may be different from that of bending roll pipe piers. Regarding hollow spiral steel pipe piers, the experimental and numerical studies were conducted in the previous studies (Ono et al. 2008; Ohnishi et al. 2011). The seismic performance and seismic evaluation methods for hollow spiral steel pipe piers were examined. On the other hand, studies on concrete-filled spiral steel pipe piers are not sufficient. Therefore, it is very important to grasp the elasto-plastic behavior such as ultimate strength and the ductility of

[1]Associate Professor, Department of Civil Engineering, Osaka University.
[2]Professor, Department of Civil and Environmental Engineering, Waseda University.
[3]Senior Researcher, National Institute for Land and Infrastructure management, Ministry of Land, Infrastructure, Transport and Tourism.
[4]Engineer, IHI Infrastructure Systems Co., Ltd.

concrete-filled spiral steel pipe piers.

In this study, in order to grasp the elasto-plastic behavior of concrete-filled spiral steel pipe piers, cyclic loading experiments were conducted. On the basis of the experimental results, seismic performance such as the ultimate strength and the ductility and seismic evaluation methods as for concrete-filled spiral steel pipe piers were investigated.

Outline of Experiments

(1) Test Specimens

In this investigation, four test specimens were employed. The outline of the dimensions of test specimen is given in Figure 1 and the values of dimension are major parameters of the test specimens are listed in Table 1. The test specimens were made of SKK490. SKK490 has been usually employed as steel tube piles. The test specimens that are called 'P9' and 'P7' are test specimens without concrete. The test specimens that are called 'C9' and 'C7' are concrete-filled test specimens. The values of the radius thickness ratio parameter applied to each specimen are different. The plate thicknesses of test specimens 'P9' and 'C9' is 9mm and that of test specimens 'P7' and 'C7' is 7mm. As for concrete-filled test specimens 'C9' and 'C7', test specimens were filled with concrete from the base section to 1,350mm as shown in Figure 1. This height of concrete satisfies the condition that the stress of steel section at the top of filled concrete does not exceed yield stress or the local buckling does not occur at this section. R_t is a radius thickness ratio parameter. λ is a slenderness ratio parameter of the column. The definitions of parameters mentioned above are identical to those stipulated in the 2012 design specifications (Japan Road Association 2012a; Japan Road Association 2012b) and given as follows.

$$R_t = \sqrt{3\left(1-\nu^2\right)}\frac{\sigma_y}{E}\frac{D}{2t} \tag{1}$$

$$\bar{\lambda} = \frac{1}{\pi}\sqrt{\frac{\sigma_y}{E}}\frac{2h}{r} \tag{2}$$

where D = diameter; t = plate thickness; σ_y = yield stress; E = Young's modulus; ν = Poisson's ratio; h= column height (distance from the bottom of the column to the point of application of horizontal load); r = radius of gyration of cross section.

(2) Loading Condition

Loading condition is shown in Figure 2. In Figure 2, 'N' indicates the axial force and 'P' indicates the horizontal load. Each specimen was loaded with hydraulic jacks that were installed in a fully stiff frame. In each experiment, the specified axial force as shown

in Table 1 was first applied to the specimen by the vertical hydraulic jack. The axial force in Table 1 is 15% of yield axial force calculated using the nominal yield stress.

The cyclic pattern of the horizontal displacement is schematically shown in Figure 3, where δ_{yN} is calculated by the following equation. The axial load was kept constant during each experiment.

$$P_{yN} = \left(\sigma_{yN} - \frac{N}{A} \right) \frac{Z}{h} \tag{3}$$

$$\delta_{yN} = \frac{P_{yN} h^3}{3EI} \tag{4}$$

where σ_{yN} = nominal yield stress; N = axial load; I = moment of inertia; Z = section modulus.

Experimental Results and Comments

Figure 4 shows horizontal load - horizontal displacement (P-δ) relationship and Figure 5 shows the envelope curves gained from the P-δ relationship. Figure 6 expresses the normalized envelop curves. The major values of experimental results are shown in Table 2.

In Table 2, $P_{\max}$ is a maximum horizontal load and δ_m is a horizontal displacement at $P_{\max}$. In Figure 6, P_{yM} of test specimens 'P9' and 'P7'is a yield horizontal load calculated by Eq. (3) with σ_{yM} instead of σ_{yN}. δ_{yM} of test specimens 'P9' and 'P7' is a yield horizontal displacement calculated by Eq. (4) with P_{yM} instead of P_{yN}. P_{yM} and δ_{yM} of test specimens 'C9' and 'C7' are a yield horizontal load and a yield horizontal displacement calculated by M-φ models shown in Figure 7. The triangular symbols (▲) in Figures 4, 5 and 6 express the points where $P_{\max}$ was observed.

As shown in Figure 4 and Figure 5 or Table 2, filling spiral steel pipe piers with concrete leads the increase in $P_{\max}$ and δ_m of spiral steel pipe piers. According to Figure 6, $P_{\max}/P_{yM}$ and δ_m/δ_{yM} of 'P9' are larger than those of 'P7'as for hollow spiral steel pipe piers. On the other hand, $P_{\max}/P_{yM}$ and δ_m/δ_{yM} of 'C9' are the almost same as those of 'C7' as for concrete-filled spiral steel pipe piers. The values of the radius thickness ratio parameter 'R_t' of 'P9' and 'C9' are smaller than those of 'P7' and 'C7'. This fact indicates that the influence of the radius thickness ratio parameter on the ultimate strength and the ductility of concrete-filled spiral steel pipe piers is smaller than that of hollow spiral steel pipe piers. The tendency agrees with that of bending roll steel pipe piers (Public Works Research Institute et al. 1997-1999).

Applicability of the Previous Seismic Evaluation Method

The comparison of experimental results of spiral steel pipes in this study with the previous experimental results of concrete-filled steel piers and the calculation results by the previous seismic evaluation method for concrete-filled steel bridge piers described in the seismic design specifications in order to verify whether the previous seismic design method can be applied to concrete-filled spiral steel pipe piers. $P_{\max}$ and δ_m were focused on as indexes for confirming the applicability of the previous evaluation method to the concrete-filled spiral steel pipe piers. The seismic evaluation method described in the 2012 seismic design specifications for highway bridges (Japan Road Association 2012b) was adapted as the previous seismic evaluation method.

In the 2012 seismic design specifications, the M-φ model as shown in Figure 7 is stipulated for evaluating seismic performance of concrete-filled steel bridge piers. The M-φ model is decided based on the experimental results of concrete-filled bending roll pipes as for pipe section steel bridge piers (Public Works Research Institute et al. 1997-1999). The point (φ_a, M_a) of the M-φ model in Figure 7 corresponds to the point (δ_m , $P_{\max}$) in Figure4 and Figure 5. The following procedure is a method how to set the M-φ model for concrete-filled steel bridge piers with circular section.

1) The stress-strain curves for steel and concrete shown in Figure 8 are assumed as a stress-strain curve for setting the M-φ model.
2) Allowable strain 'ε_a' corresponding to the point (φ_a, M_a) for concrete-filled steel bridge piers with circular section is obtained by using following equation.

$$\varepsilon_a = 5\varepsilon_y \tag{5}$$

where ε_y = yield strain of the steel used in the target steel pier.
Here, the above Eq. (5) can be applied if the following condition is satisfied.

$$0.03 \leq R_t \leq 0.12,\ 0.2 \leq \overline{\lambda} \leq 0.4,\ 0.0 \leq N/N_{yN} \leq 0.2 \tag{6}$$

3) The point (φ_y, M_y) is determined by taking the smaller one of (φ_{yc}, M_{yc}) and (φ_{yt}, M_{yt}). The points (φ_{yc}, M_{yc}) and (φ_{yt}, M_{yt}) are set when the strain in the center of plate thickness at the compression side or the tension side reaches the yield strain ε_y of steel for the first time respectively.
4) The point (φ_a, M_a) is set when the strain in the center of plate thickness at the compression side reaches the allowable strain ε_a obtained from the Eq. (5) for the first time.

$P_{\max}$ is calculated by dividing M_a by the load height h and δ_a is calculated by utilizing the curvature distribution, ignoring shear deformation and geometric non-linearity effect.

Figure 9 shows the comparison of experimental results of concrete-filled spiral steel pipes in this study ('●' in Figure 9) with the previous experimental results of concrete-filled steel piers and the calculation results by the previous seismic evaluation

method described in the 2012 seismic design specifications. The previous experimental results shown in Figure 9 include not only the results of concrete-filled steel bridge piers with pipe section but also those of concrete-filled steel bridge piers with box section. The empty circular symbols '○' indicate results of pipe section and the empty square symbols '□' indicate those of box section.

As shown in Figure 9, relatively good agreement between the experimental results of concrete-filled spiral steel pipes in this study and calculation results by the previous seismic design method can be found. The relationship between the calculation results by the previous seismic evaluation method and the experimental results of concrete-filled spiral steel pipe piers is basically similar to that between the calculation results and the previous experimental results of concrete-filled steel bridge piers with pipe section and box section. This fact indicates the possibility that the seismic evaluation method for concrete-filled bending roll pipe piers can be applied to the concrete-filled spiral steel pipe piers.

Conclusions

In this study, cyclic loading experiments were carried out in order to grasp the elasto-plastic behavior of the concrete-filled spiral steel pipe piers and to investigate the applicability of the previous seismic evaluation method to the concrete-filled spiral steel pipe piers. The major results gained from this study are concluded as follows.

- Filling spiral steel pipe piers with concrete leads the increase in the ultimate strength and ductility of spiral steel pipe piers.
- The influence of the radius thickness ratio parameter on the ultimate strength and the ductility of concrete-filled spiral steel pipe piers is smaller than that of hollow spiral steel pipe piers.
- The comparison between the experimental results and the calculation results by the previous seismic evaluation method indicates that the seismic evaluation method for concrete-filled bending roll pipe piers can be applied to the concrete-filled spiral steel pipe piers.

References

Kiyoshi Ono, Mitsuyoshi Akiyama and Atsushi Yabumoto (2008). EXPERIMENTAL STUDY ON SEISMIC PERFORMANCE OF SPIRAL STEEL PIPES, Proceedings of the 24th US-Japan Bridge Engineering Workshop, pp.411-419.

Japan Road Association (2012a). *Specifications for highway bridges, Part II: Steel bridges* (in Japanese).

Japan Road Association (2012b). *Specifications for highway bridges, Part V: Seismic Design* (in Japanese).

Public Works Research Institute of the Ministry of Construction and five other

organizations (1997-1999). “Ultimate Limit State Design Method of Highway Bridges Piers under Seismic Loading”, *Cooperative Research Report* (in Japanese).
Shohei Ohnishi, Kiyoshi Ono and Mitsuyoshi Akiyama (2011). ANALYTICAL STUDY ON SEISMIC PERFORMANCE OF HOLLOW SPIRAL STEEL PIPES UNDER CYCLIC LOADING, Procedia Engineering, Vol.14 , pp.898-905.

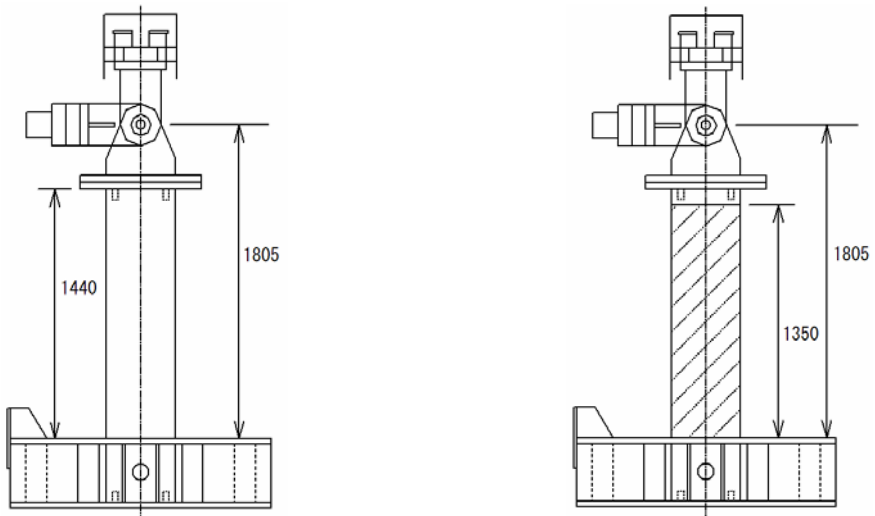

(a) Hollow test specimens (P9, P7) (b) Concrete-filled test specimens (C9, C7)

Figure 1 Test Specimens

Table 1 Dimension and Parameters of Test Specimens

		P9	C9	P7	C7
Concrete		unfilled	filled	unfilled	filled
Compressive Strength (MPa)			18.9		19.6
Material (JIS)		SKK490			
Diameter (mm)		400		400	
Thickness (mm)		9		7	
Radius Thickness ratio		22.2		28.6	
Area (cm^2)		111		86	
Moment of inertia (cm^4)		21,138		16,691	
The Height of Loading point (mm)		1,805		1,805	
Compressive Axial Force (kN)		524		408	
Parameters calculated by nominal yield stress σ_{yN}	λ	0.33		0.32	
	R_t	0.056		0.072	
Parameters calculated by experimental yield stress σ_{yM}	σ_y (MPa)	470		409	
	λ	0.40		0.37	
	R_t	0.084		0.093	

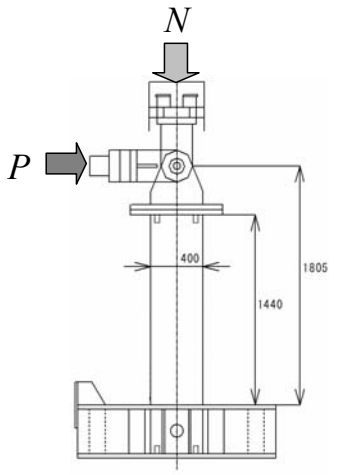

(unit: mm)

Figure 2 Test Setup

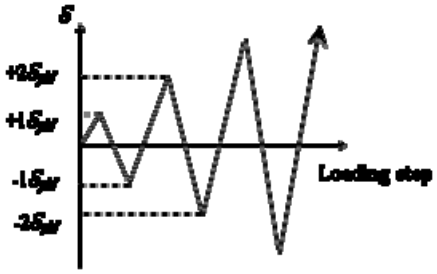

Figure 3 Cyclic Loading Pattern

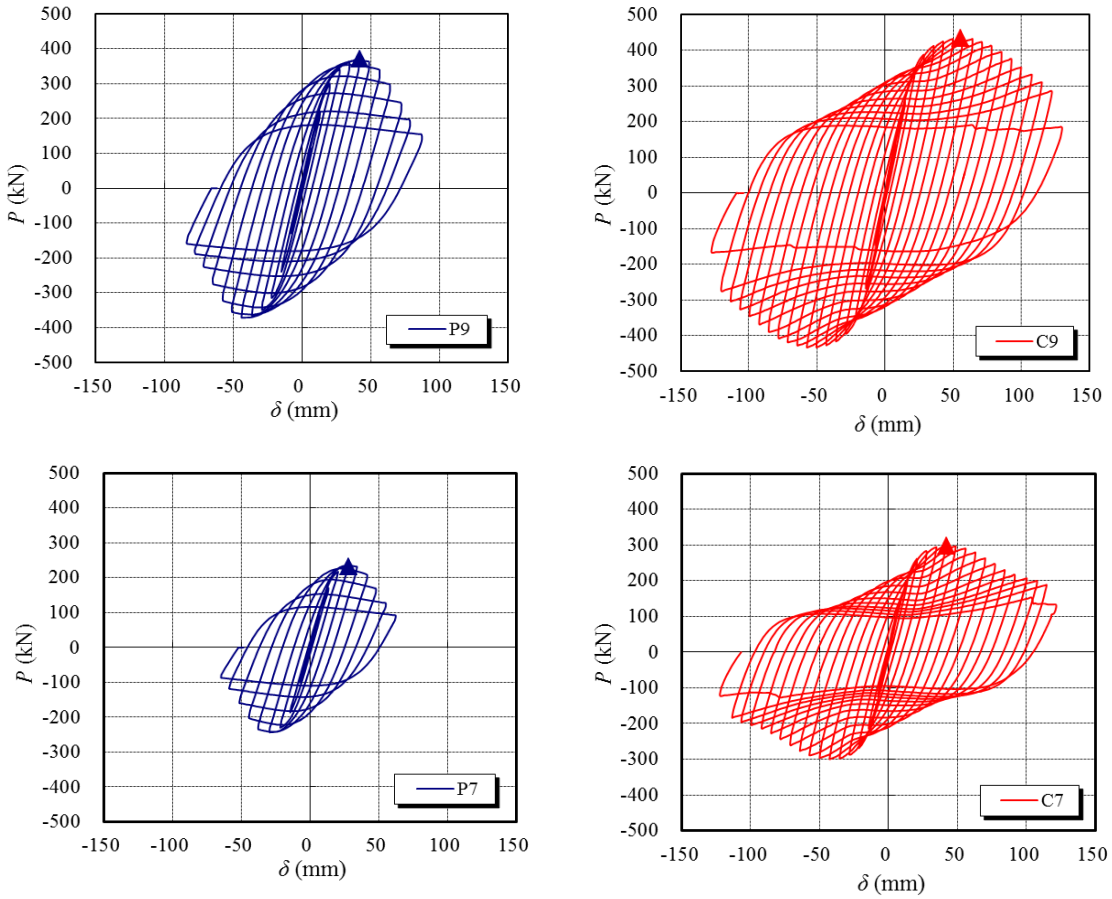

Figure 4 *P-δ* Relationship

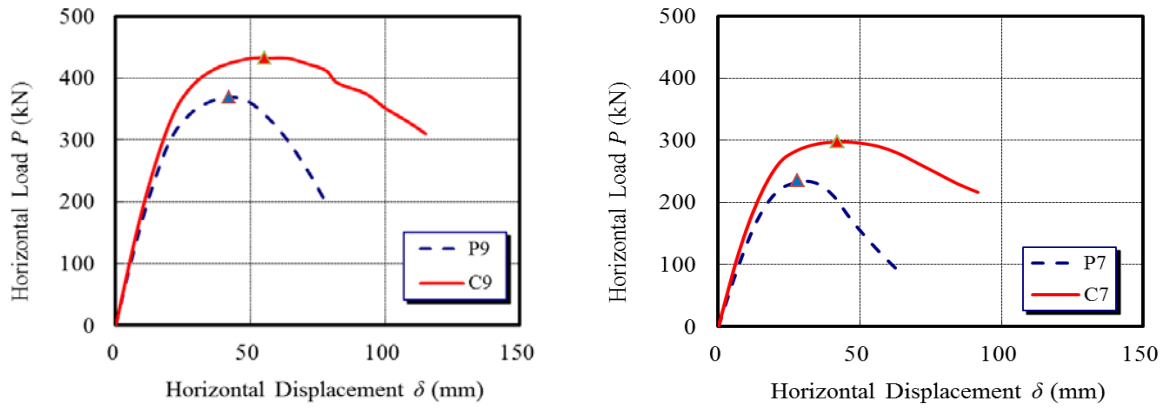

Figure 5 Envelop Curves

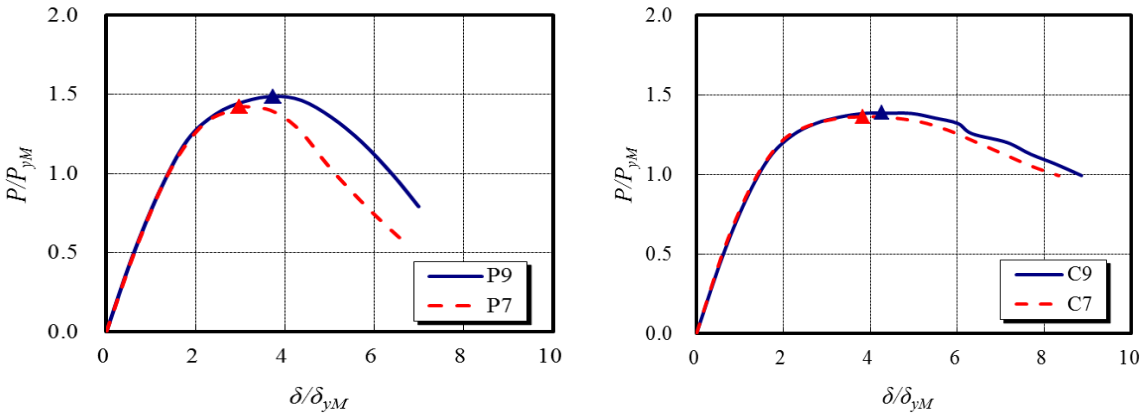

Figure 6 Normalized Envelop Curves

Table 2 Experimental Results

Test Specimen	P9	C9	P7	C7
P_{max} (kN)	369	433	231	297
δ_m (mm)	42.0	55.3	28.1	42.1

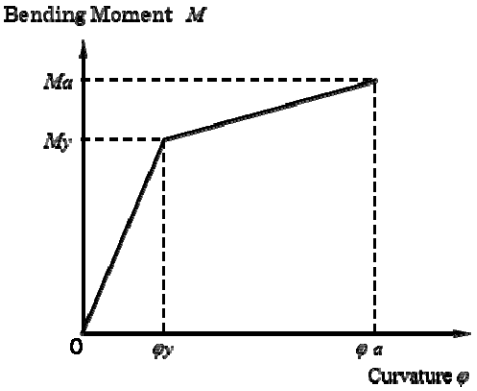

Figure 7 *M-φ* Model

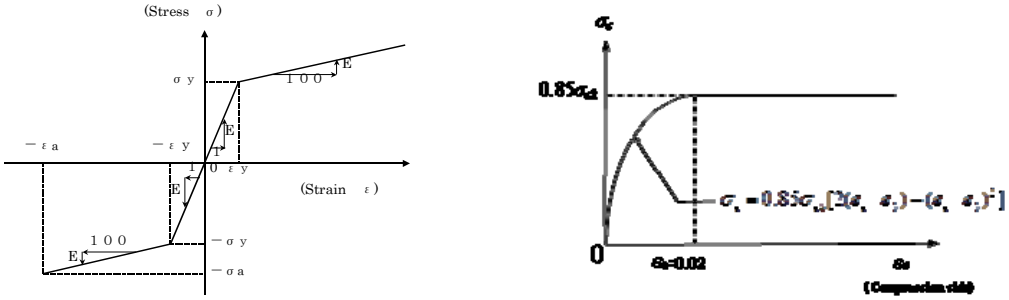

(a) Steel **(b) Concrete**

Figure 8 Stress-Strain curves

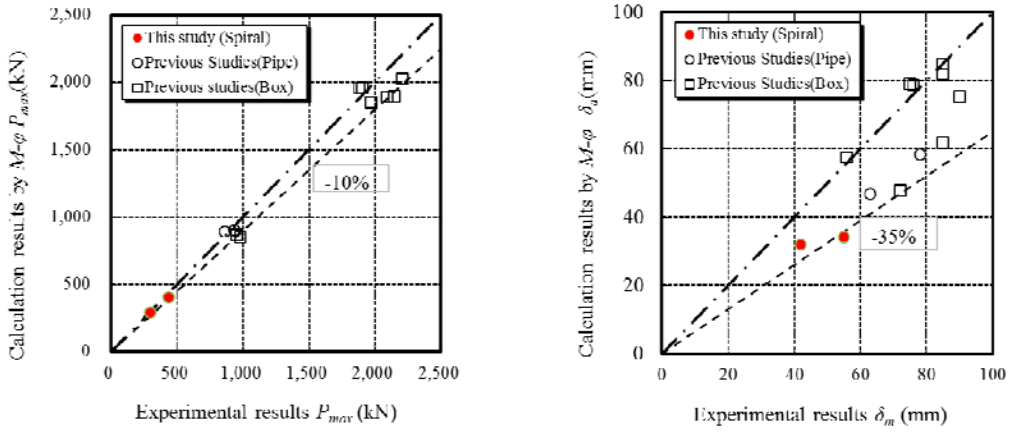

(a) P_{max} (b) δ_m

Figure 9 Comparison between Experimental Results and Calculation Results